COMPARING THE BEHAVIOR OF SIMULATED PROTON SYNCHROTRON RADIATION IN THE ARCS OF THE LHC WITH MEASUREMENTS*

G. Guillermo†,[1], Cinvestav, Mérida, México
M. Ady, R. Kersevan, F. Zimmermann, CERN, Geneva, Switzerland
D.C. Sagan, Cornell U., Ithaca N.Y., U.S.A
E. La Francesca[2], M. Angelucci, R. Cimino, LNF, Frascati, Italy
[1]also at CERN, Geneva, Switzerland
[2]also at University "Sapienza" , Roma, Italy

Abstract

In previous work it was shown that at high proton-beam energies, synchrotron radiation is an important source of beam-screen heating, of beam-related vacuum pressure increase, and of primary photoelectrons, which can contribute to electron-cloud formation. We have used the Synrad3D code developed at Cornell to simulate the photon distributions in the arcs of the LHC, HL-LHC, and FCC-hh. In particular, for the LHC we studied the effect of the 'sawtooth' chamber. In this paper, specific results of the Synrad3D simulations are compared with simulations by another code, Synrad+, developed at CERN, and with experimental data from a synchrotron-light beam line at BESSY II for actual LHC vacuum-chamber samples.

INTRODUCTION

In previous work [1], using the tool Synrad3D [2], we studied the efficiency of the sawtooth pattern imprinted on the outer side of the vacuum wall at the arcs of the LHC. These Synrad3D simulations confirmed that the sawtooth greatly reduces the amount of photoelectrons finally absorbed at either the bottom or top of the chamber, by almost a factor of 10, from 33% to 4% (sum of top and bottom), as had been its purpose. In the present work we first benchmark the tool Synrad3D against a different program called Synrad+, and then compare its prediction with experimentally obtained photon reflectivities for different photon energies and angles of incidence, measured on LHC beam-screen sample surfaces in a synchrotron-light beam line at BESSY II. It has been shown that at-wavelength synchrotron radiation reflectivity measurements can give important parameters to perform simulations of realistic systems [3–7]. The reach of such experimental approach recently received a significant boost once the new metrology station become available at BESSY II [8]. The new setup allows to study reflectivity and photon yields at very grazing incident angles (in some cases below 0.5°) in the 36-1800 eV region.

* This work was supported by the Mexican CONACyT "BEAM" Programme, INFN- NCV project MICA, and also by the European Commission under the HORIZON2020 Integrating Activity project ARIES, grant agreement 730871

† gerardo.guillermo.canton@cern.ch

Synrad3D and Synrad+

Synrad3D [2] was developed at Cornell U. by D. Sagan and G. Dugan. Our previous simulation results obtained with Synrad3D [1] can be benchmarked against another code, Synrad+ [9].

Synrad+, like Synrad3D, is a Monte Carlo simulator for synchrotron radiation, developed since the 1990s. With Synrad+ the user can define the beam properties and magnetic regions, typically representing dipoles or quadrupoles. The software then calculates the beam trajectory and generates virtual photons distributed evenly along the beam path inside the magnetic region. These photons are then traced in a geometry described by polygons, that can be described inside the code or imported from external CAD programs. Due to the 3D visualization and since geometries of arbitrary complexity can be treated, Synrad+ is suitable for detailed simulations of accelerator components. Since the number of polygons is limited to a few hundred thousands, however, Synrad+ cannot simulate large (e.g., several km long) machines without significant simplifications of the geometry.

Although in principle one should be able to use either code for any synchrotron radiation analysis, we find that Synrad3D is much more practical for complex or long lattices, while Synrad+ is better suited at treating difficult and irregular chambers, such as places where BPMs are installed.

CODE COMPARISON

As in Ref. [1], we consider the optical lattice of an LHC arc cell arcs at top energy, i.e. 7 TeV. One optical arc cell consists of two halves with three bending magnets each. We limited our simulations to synchrotron radiation emitted while passing through the fields of these dipoles. We started by comparing the emission mechanisms, and then moved into the tracking of photons through all reflections till final absorption; for each case 0.2 million photons were tracked using Synrad3D and 100 million with Synrad+.

For the first part we defined the wall as a perfect absorber, so that the absorption points would depend solely on the emission, and we used an ideal beam with zero emittance. Figure 1 shows the absorption of photons along the coordinate s as determined by both codes.

Next, we included the size of the beam and the material properties of the chamber wall in the simulation. We con-

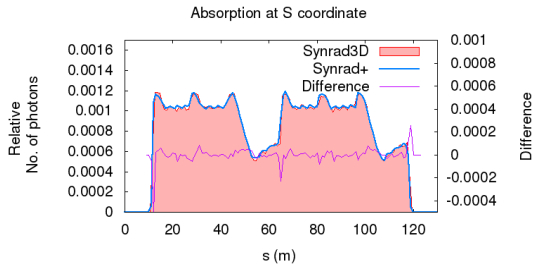

Figure 1: Simulated photon absorption as a function of longitudinal coordinate s for one LHC arc cell, treating the chamber wall as a perfect absorber; the blue line is the result using Synrad+, while the red area is the result from Synrad3D.

sidered a copper wall, without any carbon coverage on the surface, with a surface roughness of 40 nm. In addition, the sawtooth pattern on the horizontally outward side of the vacuum chamber was included. For this simulation model, the absorption points along the coordinate s obtained from each code are compared in Fig. 2.

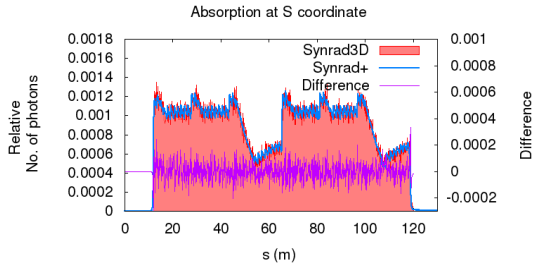

Figure 2: Comparison of photon absorptions as a function of s simulated by Synrad+ and Synrad3D, for the realistic model of the beam pipe.

MEASUREMENTS

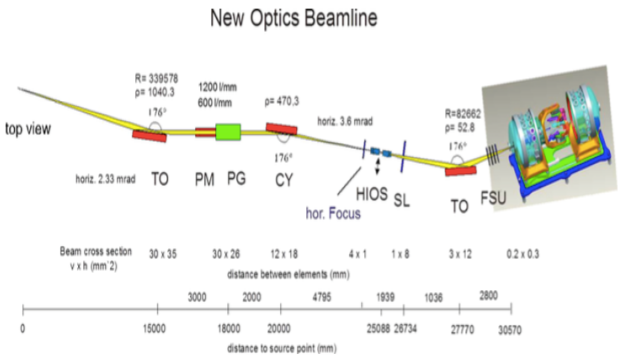

Figure 3: BESSY II optics beamline [8].

The reflectivity measurements were performed at BESSY II. The general experimental setup is described in Refs. [8] and [10], as schematically shown in Fig. 3. Synchrotron radiation coming from BESSY II is made monochromatic through a plane grating monochromator (PM-1) with a blazed gratings (1200 l/mm), before arriving to the end station. In this configuration, it is possible to vary the photon energy from 35 to 1800 eV, the incidence angle from 0° to 90° and the detectors position from 0° to 180° with respect to the optical axes, collecting the specular and non-specular reflections. The accuracy of the specular reflection measurement depends on the purity of the monochromatic light in the BESSY II beam line; a conservative error estimate is 10^{-5}. The error of total reflectivity measurements for a rough surface can be 100 times larger. Our measurements were performed on two different samples: a smooth copper surface, with a roughness of $R_a = 9.6$ nm, and a 10 cm piece of a chamber, shown in Fig. 4, with the actual sawtooth pattern used for the LHC beam screen.

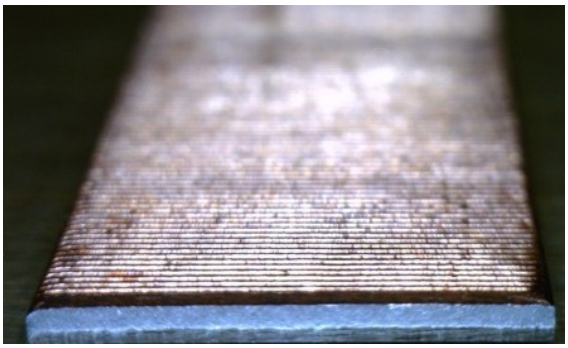

Figure 4: Cu sawtooth sample.

The measured specular reflectivity for the smooth copper sample, with an incident angle spanning from 0.25° to 7°, is reported in Fig. 5 and the simulated total reflectivity (i.e. the sum of specular and diffuse reflection) in Fig. 6. These two results agree rather well. In fact, for close to ideal mirror-like surfaces the total reflectivity computed by Synrad3D is essentially all in the forward direction and, in this particular case, directly comparable with the experimental measurements of specular reflectivity as shown in Fig. 5. This would no longer be true for rough surfaces where the forward reflected component is only a fraction of the total reflectivity.

Certainly this correspondence is not fulfilled for the sawtooth structure, illustrated in Fig. 4. In Fig. 7 we present the measured forward reflectivity for two angles of incidence, 1° and 2°, for the sawtooth sample. The value of the measured forward reflectivity is much reduced compared with the specular reflectivity observed for a smooth surface; compare for example the curve for 50 eV in Fig. 5. The sawtooth structure was indeed introduced to reduce forward reflectivity to mitigate the electron-cloud build up due to photoelectrons [4, 6, 11].

The curves in Fig. 8 represent the simulated total reflectivity. The measured forward reflectivity of Fig. 7 is significantly lower than the total simulated reflectivity as would be expected for an artificially rough surface.

At three photon energies (36, 45 and 100 eV), and two different angles of incidence (1° and 2°), we measured the entire photon distribution over a significant solid angle. An experimental estimate of the total reflectivity was obtained by numerical integration of all forward, diffused and back reflected photons over the available solid angle. Figure 8 includes these six measurement points of total reflectivity for the sawtooth chamber (the dots), revealing a higher total reflectivity than expected from the simulation model. In particular, the simulated reflectivity decreases by more than a factor of 10 as the photon energy increases from 35 eV to 100 eV, while the measured reflectivity at 35 eV is about 2 times larger than the simulated value, and remains almost constant for higher photon energies. Both simulated and measured reflectivities weakly depend on the (small) angle of incidence.

The measured data demonstrate the ability of the BESSY II system to distinguish between forward, diffused and back reflected photons, representing an ideal test bench to verify simulation codes.

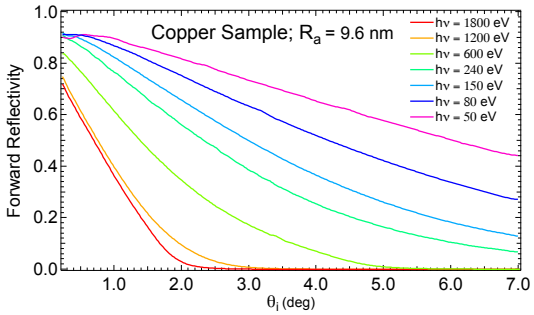

Figure 5: Measured normalized reflectivity vs. incidence angle for different energies for a copper surface, for different photon energies.

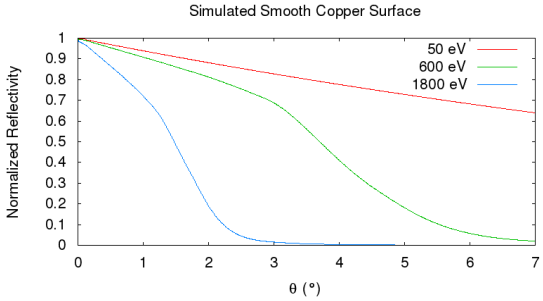

Figure 6: Simulated normalized total reflectivity vs. incidence angle for different energies for a copper surface, for different photon energies.

DISCUSSION

Synrad+ and Synrad3D produce nearly identical simulation results for the photon flux in an LHC arc cell. This was almost expected since the surface model used in the two codes is rather similar, and they used the same reflectivity

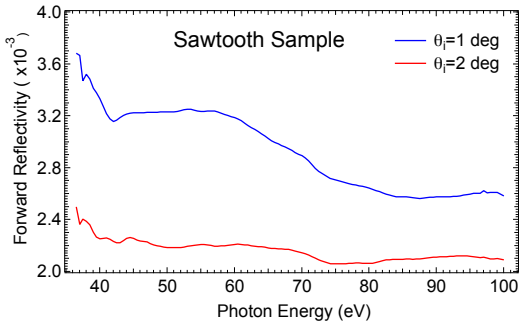

Figure 7: Measured normalized forward reflectivity as a function of the energy of impinging photons (36 eV - 100 eV), for two different incidence angles on a sawtooth chamber.

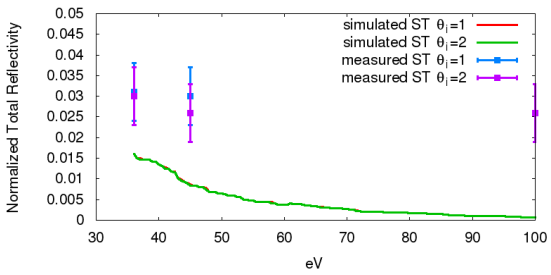

Figure 8: Simulated normalized total reflectivity as a function of the energy of impinging photons (36 eV - 100 eV), for two different incidence angles on a sawtooth chamber.

tables. The primary differences between the two codes are the modeling of the beam-pipe boundaries and the approximation used for the sawtooth pattern.

Comparing Synrad3D simulations with photon reflectivity measurements at BESSY II, we observe a fairly good agreement in the specular photon reflectivity, even in absolute value, between the predictions from Synrad3D and the experimental results for flat samples. According to both simulations and measurements, for the sawtooth pattern, the specular (forward) reflectivity is much reduced, at the expense of increased diffuse scattering and backscattering. However, the simulated total reflectivity is significantly lower than the measured total reflectivity and decreases much more strongly with photon energy. This qualitative difference might be due to differences between the manufactured sawtooth and the idealized model used in the simulation.

The results reported here represent work in progress. In the future we plan to refine the sawtooth model used in the simulation, to take and analyze more experimental data, including at larger angles of incidence and higher photon energies, and to proceed with this benchmarking of measurements and simulations.

ACKNOWLEDGMENTS

We thank HZB for the allocation of synchrotron radiation beam time and E.LF. and M.A. thankfully acknowledge their financial support.

REFERENCES

[1] G. Guillermo Cantón, D. Sagan and F. Zimmermann, "Simulating Proton Synchrotron Radiation in the Arcs of the LHC, HL-LHC and FCC-hh," in *Proc. of Int. Particle Accelerator Conf.*, pp. 2073–2076, JACoW, June 2016.

[2] G. Dugan and D. Sagan, "Simulating synchrotron radiation in accelerators including diffuse and specular reflections," *Phys. Rev. Accel. Beams*, vol. 20, p. 020708, Feb 2017.

[3] R. Cimino *et al.*, "Vacuum chamber surface electronic properties influencing electron cloud phenomena," in *App. Surf. Sci.*, p. 231 vol. 235, Jul 2004.

[4] N. Mahne *et al.*, "Photon reflectivity distributions from the LHC beam screen and their implications on the arc beam vacuum system," in *App. Surf. Sci.*, vol. 235, p. 221, Jul 2004.

[5] G. F. Dugan *et al.*, "Measurements of x-ray scattering from accelerator vacuum chamber surfaces, and comparison with an analytical mode," in *Phys. Rev. ST Accel. Beam*, vol. 18, p. 040704, Jul 2015.

[6] R. Cimino *et al.*, "Electron cloud in accelerator," in *Int. J. of Modern Physics A*, vol. 29, p. 1430023, Jul 2014.

[7] F. Schäfers and R. Cimino, "Soft x-ray reflectivity: from quasi-perfect mirrors to accelerator walls," in *Proc. ECLOUD'12, CERN Yellow Report CERN-2013-002*, vol. 29, p. 105, Jul 2013.

[8] A. A. Sokolov, F. Eggenstein, A. Erko, R. Follath, S. Künstner, M. Mast, J. S. Schmidt, F. Senf, F. Siewert, T. Zeschke, and F. Schäfers, "An XUV optics beamline at BESSY II," in *Proc. SPIE*, vol. 9206, p. 92060J, Sept. 2014.

[9] R. Kersevan, "Synrad, a Monte Carlo synchrotron radiation ray-tracing program," in *Proc. of Int. Conf. on Particle Accelerators*, pp. 3848–3850 vol. 5, May 1993.

[10] F. Eggenstein, P. Bischoff, A. Gaupp, F. Senf, A. Sokolov, T. Zeschke, and F. Schäfers, "A reflectometer for at-wavelength characterization of XUV-reflection gratings," in *Proc. SPIE*, vol. 9206, p. 920607, Sept. 2014.

[11] O. Gröbner, "Technological problems related to the cold vacuum system of the LHC," in *Vacuum*, vol. 47, pp. 591–595, 1996.